Applied Surface Science 255 (2008) 2874–2878

Contents lists available at ScienceDirect

Applied Surface Science

journal homepage: www.elsevier.com/locate/apsusc

Formation of mesoporous alumina via hydrolysis of modified aluminum isopropoxide in presence of CTAB cationic surfactant

Kamal M.S. Khalil *

Chemistry Department, Faculty of Science, Sohag University, P.O. Box 82524, Sohag, Egypt

ARTICLE INFO

Article history:
Received 30 December 2007
Received in revised form 20 June 2008
Accepted 17 August 2008
Available online 4 September 2008

Keywords:
Alumina
Cationic surfactant
CTAB
Sol–gel
Mesoporous

ABSTRACT

Formation of mesoporous alumina at room temperature via combined utilization of acetic acid (as an organic modifier) and cetyl trimethyl ammonium bromide (CTAB) as a cationic surfactant has been investigated in n-heptane medium. The reactants molar ratio was aluminum isopropoxide:acetic acid:water:CTAB:n-heptane, as 1:1:3:*x*:15, where *x* was 1 or 3. The calcined materials (at 600 °C for 3 h) were characterized by Fourier transform infrared (FTIR) spectroscopy, X-ray diffraction (XRD) and N_2 adsorption/desorption techniques. Thus, amorphous (weakly crystalline γ-phase) mesoporous aluminas of possible hexagonal symmetry, high surface area and relatively narrow pore size distribution were obtained. The enhancement of surface area and retardation of crystallization were found to increase with the increasing of CTAB ration in the reaction mixture.

1. Introduction

Mesoporous alumina is an essential material for vast number of technological applications [1,2]. However, on comparison with mesoporous silica, mesoporous alumina normally shows less order, lower thermal stability and often broad pore size distribution, which is a major drawback for many applications [3]. Therefore, extensive efforts have recently been directed toward the synthesis of nanostructured alumina with ordered mesoporous structure. Many synthetic strategies have been developed based on surfactant assisted (template) sol–gel methods and organic additives [3,4]. Calcination of the produced materials at ≥500 °C normally leads to the formation of thermally stable mesoporous alumina. Preparation of mesoporous aluminas using template-free solvothermal [5] and microemulsions [6] approach have also been reported.

Investigations based on the surfactant-assisted approach have involved different anionic [4,7–11], cationic [4,12–15] and neutral [16,17] surfactants. Thus, hexagonal alumina mesophase were obtained by using of anionic surfactants such as sodium dodecyl sulphate [7,10,11]. However, because of the difficulties in removing the anionic group without destroying the pore structure, this path is not welcomed [3]. On the other hand, cetyl trimethyl ammonium bromide (CTAB) was the most employed cationic surfactant for the preparation of ordered mesostructured aluminas either via sol–gel processing or homogenous precipitation [12–15] at some elevated temperatures.

Moreover, investigations based on the organic additive approach have involved glucose [18], hydro-carboxylic acid [19], and diketones [20]. Thus, alumina mesophases were obtained by reacting aluminum alkoxides and carboxylic acids with controlled amounts of water in low-molecular-weight alcoholic solvents [21]. The combined utilization of surfactants and urea modifiers has also been investigated [22].

However, while most of the surfactant assisted approach methods require processing at high temperature or hydrothermal processing, and utilization of carboxylic acids produces ordered materials for C_4 and higher acids at high temperature [21]. The present article reports a simple method for the formation of mesoporous alumina at room temperature. The method is based on the hydrolysis of aluminum isopropoxide modified with acetic acid in presence of CTAB as a cationic surfactant and n-heptane as a solvent. Characterization results for the test materials via thermogravimetric analyser (TGA), differential scanning calorimeter (DSC), Fourier transform infrared (FTIR) spectroscopy, small as well as normal angle X-ray diffraction (XRD), and analysis of nitrogen adsorption/desorption isotherms are presented.

* Tel.: +20 121 138 223; fax: +20 934 601 159.
E-mail address: kms_khalil@yahoo.co.uk.

0169-4332/$ – see front matter © 2008 Elsevier B.V. All rights reserved.
doi:10.1016/j.apsusc.2008.08.091

2. Experimental

2.1. Materials

2.1.1. Chemicals

Aluminum isopropoxide, Aldrich; acetic acid, Sigma–Aldrich; CTAB, 98% Aldrich; and n-heptane, >99.0%, Merck; were purchased and used as received. All preparation were carried out at room temperature and bi-distilled water was utilized.

2.1.2. Preparation of the materials

0.01 mol of aluminum isopropoxide (2.04 g) was dissolved in (0.15 mol) of n-heptane (22.0 ml), which followed by 0.01 mol (0.60 ml) of acetic acid and stirred for 1 min. To this solution, 0.03 mol (0.54 ml) of water and 0.01 (3.64 g) of CTAB were added and stirred magnetically for 1 h at 25 °C. After aging for 24 h at room temperature, the mixture was filtered without washing and dried at 60 °C for 24 h, and further at 90 °C for another 24 h. The material thus obtained is termed as uncalcined 1 mol alumina. Portion of the later material was calcined at a ramp rate of 2 °C min^{-1} up to 600 °C, then isothermally at this temperature for 3 h. The obtained calcined material is termed as calcined 1 mol alumina.

Another material was prepared by the same method where the reactants mixing ratio was as above except for CTAB where 0.03 instead of 0.01 mol was employed. The dried product for this preparation is termed as 3 mol material, and its calcinations product (obtained as above) is termed as calcined 3 mol material. One more sample was prepared by the same procedure (as for the uncalcined materials) except that there were no CTAB. This blank sample was indicated as uncalcined 0 mol alumina.

2.2. Characterization

2.2.1. Thermal analyses (TGA and DSC)

Thermal Analyses were carried out utilizing a Thermal Analyst 2000 TA instrument (USA) controlling a 2050 thermogravimetric (TG) analyzer and a 2010 differential scanning calorimeter (DSC). A platinum ceramic sample boat was used for TGA analysis. Samples weighing 10.0 ± 0.1 mg were heated up to 800 °C at 5 °C min^{-1}, in a flow (40 ml/min) of nitrogen (N_2) or oxygen (O_2) atmosphere. For the DSC measurements, aluminum open pans (without lids) were used to allow interaction of the sample with the DSC cell atmosphere, according to the instruction given in the operator's manual of the above indicated analyzer. Samples weighing 5.0 ± 0.1 mg were heated up to 550 °C at 5 °C min^{-1}, in a flow (40 ml/min) of N_2 or O_2 atmosphere, as indicated.

2.2.2. Fourier transform infrared (FTIR) spectroscopy

FTIR spectra of the KBr-supported test samples were obtained by using of a FTIR spectrophotometer, Nicolet FTIR Magna-IR 560 system (USA), in the range 4000–400 cm^{-1}, with 40 scans and a resolution of 4 cm^{-1}.

2.2.3. X-ray diffraction (XRD)

XRD patterns were obtained at room temperature. Diffraction patterns were obtained with Ni-filtered Cu Kα radiation (λ = 0.154056 nm). The patterns obtained were matched with the standard data [23] for the purpose of phase identification.

2.2.4. Nitrogen gas adsorption

Nitrogen adsorption/desorption isotherms at −196 °C were measured using a Model ASAP 2010 instrument (Micromeritics Instrument Corporation, USA) according to the standard IUPAC recommendations [24]. Prior to measurement, each sample was degassed for 2 h at 250 °C to 0.1 Pa. The specific surface area, S_{BET}, was calculated by applying the BET equation [25]. Average pore diameter was estimated by the average method from the relation 4 V_p/S_{BET}, where V_p is the total pore volume (at P/P_0 = 0.985). Pore width distribution over the mesopore range was generated by the BJH [26] analysis of the adsorption branches and value of average pore width was also estimated from the BJH distribution.

3. Results and discussion

3.1. Thermal analyses

TGA and DTG curves carried out at 5 °C min^{-1} in flow of N_2 or O_2 atmosphere for the uncalcined materials, 1 mol (N_2), 3 mol (N_2), and 1 mol (O_2) are shown in respectively in Fig. 1(a)–(c). Total weight loss values, recorded upon heating over the temperature range of RT −800 °C in flow of N_2 were 70.3%, 77.1% and 67.0%, respectively, for the uncalcined materials 1 mol (N_2), 3 mol (N_2), and 1 mol (O_2), respectively. The DTG curves suggested that weight loss process was occurred through a four steps process. It is clear that the steps limits were more sensitive for the atmosphere type than for the amount of surfactant as shown in Fig. 1(a)–(c).

In lights of the thermal analysis studies reported for similar CTAB containing systems [27], four decomposition steps can be recognized. The first step below 120 °C is assignable for the loss of the adsorbed and included water molecules and/or organics. The second and third steps together, maximize at 248, 358 °C in flow of N_2 atmosphere (or at 232 and 370 °C in flow of O_2) represent the main portion of the weight loss process (55.1% out of 70.3% in flow of N_2 (or 45.9% out of 67.0% in flow of O_2). The later two peaks, which are associated with the main portion of the weight loss process may be assigned for the removal of the template though a Hofmann degradation reaction below 250 °C and a decomposition and/or combustion reaction above 250 °C [27]. However, for the

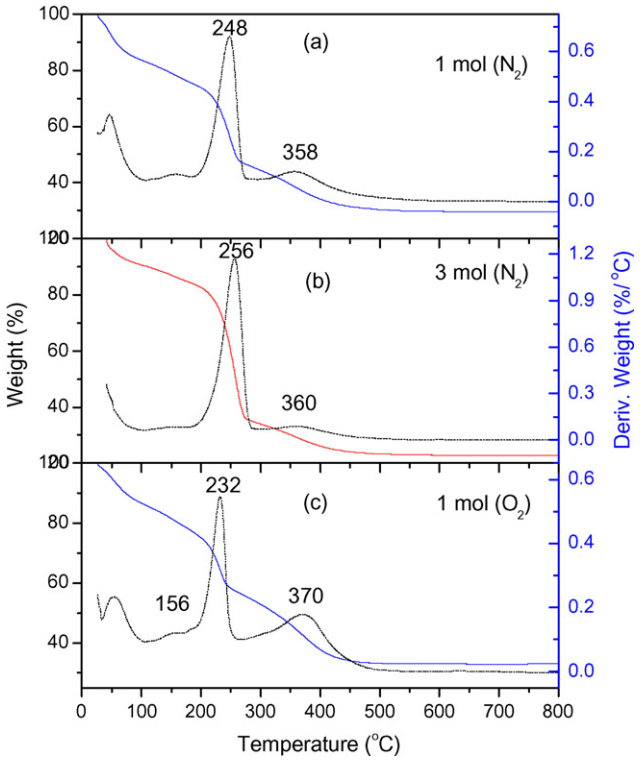

Fig. 1. TGA and DTG curves obtained for the uncalcined materials: 1 mol in flow of N_2 (a), 3 mol in flow of N_2 (b) and 1 mol in flow of O_2 (c).

present materials, the presence of acetate species must be taken in account. In lights of the fact that decomposition of acetate species is normally occur at 300–400 °C, as shown by the DSC results below. Therefore, the third step which maximize at 358 °C (N_2), or 370 °C (O_2), should be assigned for the decomposition and/or combustion of the acetate species as well as the template, too. Finally, the fourth step of the weight loss, which manifests it self above 500 °C, shows a small weight loss amounting to <0.8% either in flow of N_2 gas or O_2.

DSC results for the 1 and 3 mol materials carried out at 5 °C/min in flow of N_2 are shown in Fig. 2 (top). Two endothermic events at 104 and 245 °C, as well as two main exothermic events were observed. The first exothermic peak maximizes at 220 °C, whereas the second, maximizes at 355 and 420 °C. However, the maximum at 355 °C was more evident for the 3 mol than for 1 mol material. DSC results for the 1 and 3 mol materials in flow of O_2 atmosphere, Fig. 2 (bottom), also shows two endothermic events at 104 and 234 °C, as well as two main exothermic events. The first exothermic even is characterized by two exothermic peaks at 182 and 220 °C (instead of one peaks at 220 °C (N_2)), and the second exothermic even is characterized by two exothermic peaks at 305 and 380 °C in flow of O_2 (instead of at 355 and 420 °C (N_2)). DSC curve for an uncalcined 0 mol material (contains no surfactant) in flow of O_2 atmosphere was carried out, as shown in Fig. 2 (bottom). Curve for the 0 mol material, above 250 °C, shows only one exothermic peak at 380 °C, which is mainly due to decomposition and/or combustion of the acetate species. This proves that the peak observed at 305 °C (O_2) is originated from the template.

3.2. FTIR spectroscopy

FTIR spectra for the uncalcined materials are shown in Fig. 3. The spectra for the uncalcined alumina materials show a group of strong intense bands which can be assigned for the surfactant template as follows: the bands at 3430 cm^{-1} is assignable for to the starching modes of adsorbed water molecules. The group of bands at 2920, 2850 and 1470 cm^{-1} are assignable for the starching mode of $\nu CH(-CH_3)$ and $\nu CH(-CH_2-)$ groups and their bending mode $\delta CH(-CH_3)$ and $\delta CH(-CH_2-)$, respectively [27,28]. This confirms inclusion of the surfactants molecules. Moreover, the band at 1570 and 1420 cm^{-1} are assignable for the bonding modes of acetate group to the Al^{3+} ions (probably as a bidentate legands due to the large difference between the two bands amounts to 150 cm^{-1}). FTIR spectra of the calcined materials showed typical spectra of partially hydroxylated alumina and indicate complete removal of the bands related to the surfactant and acetate species.

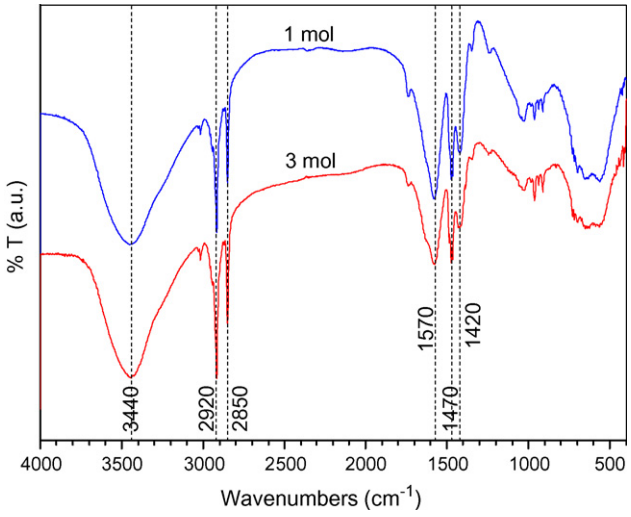

Fig. 3. FTIR spectra for the uncalcined 1 and 3 mol alumin materials as indicated.

3.3. Powder X-ray diffractometry

XRD pattern for the uncalcined modified alumina samples are shown in Fig. 4. The patterns do not show any peaks characteristic for the expected hydrolysis products that observed in absence of the surfactant, namely aluminum acetate hydroxide hydrate (AAHH, card no. 13-0834) nor boehmite, aluminum oxide hydroxide (AOH, card no. 05-0190). However, group of peak characteristics for CTAB (card no. 30-1746) was observed [23]. This

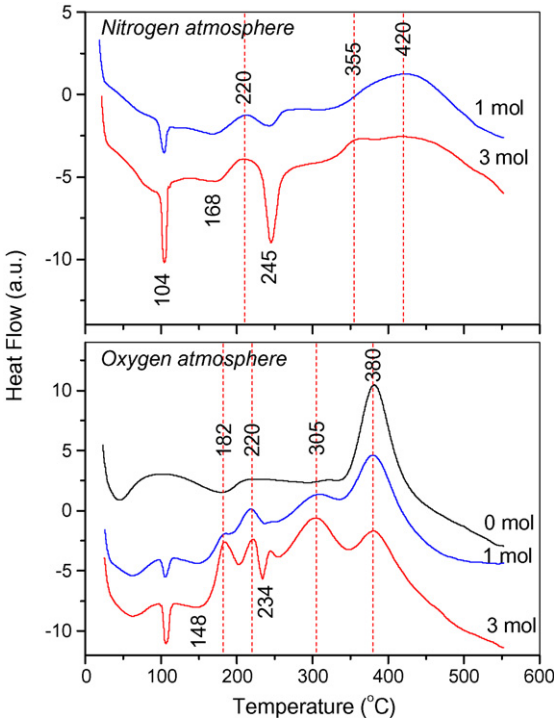

Fig. 2. DSC curves obtained for the uncalcined 1 and 3 mol materials carried for in flow of N_2 (top), and for the 0, 1 and 3 mol materials in flow of O_2 (bottom).

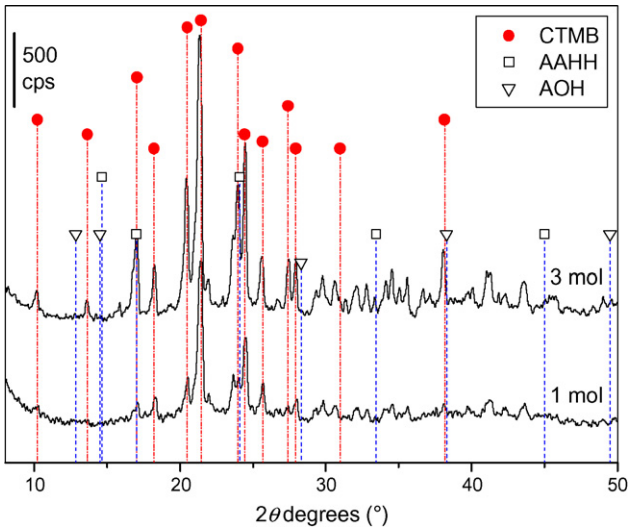

Fig. 4. XRD pattern for the uncalcined modified alumina materials.

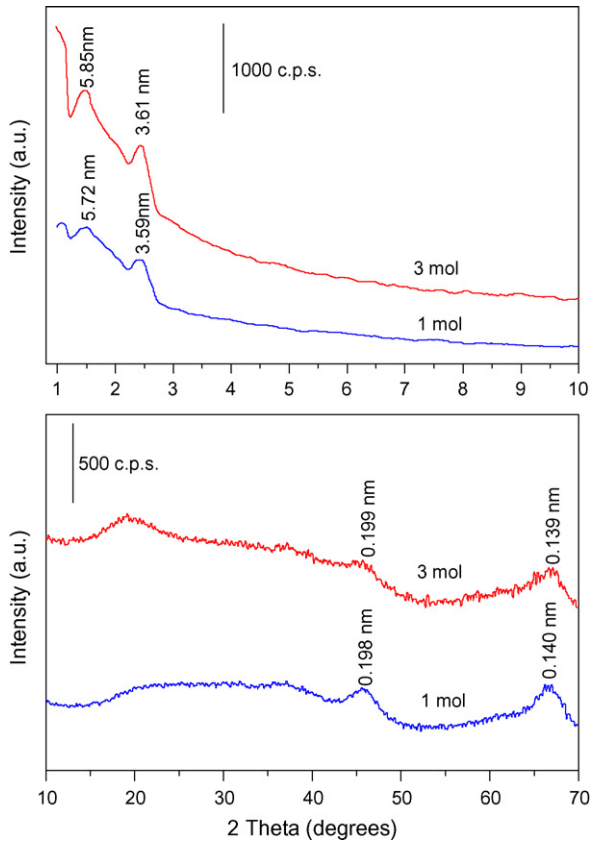

Fig. 5. Small angle (top) and high angle (bottom) XRD patterns for the calcined materials.

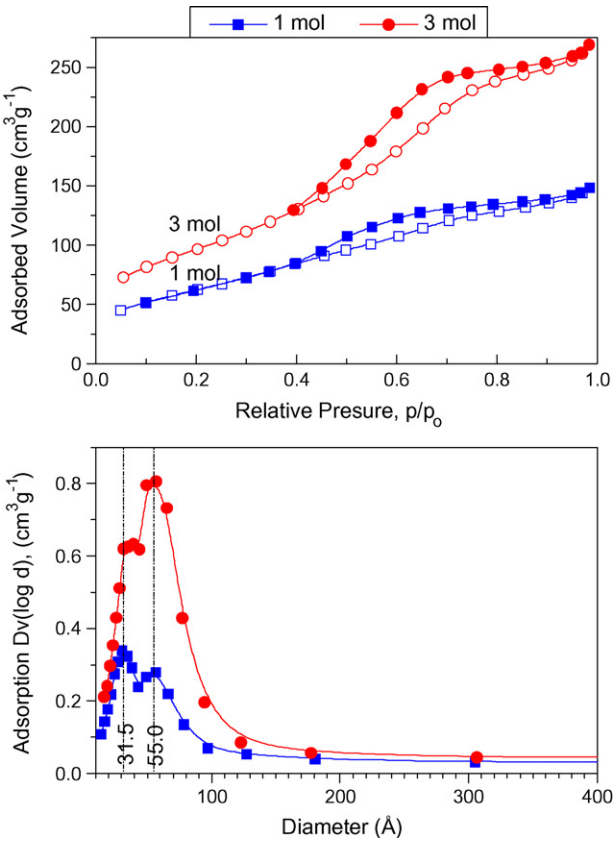

Fig. 6. Nitrogen adsorption/desorption isotherms for the 1 and 3 mol calcined materials (top), and their BJH pore width distribution (bottom).

indicates that the uncalcined modified alumina materials were amorphous and large surfactant domains were present. Fig. 5 shows small angle (top) and high angle (bottom) diffraction patterns for the calcined materials. Two XRD peaks were observed at low angles. Assuming the hexagonal lattice symmetry the two peaks may be indexed on the basis of *hkl* = 100 and 110 Bragg peaks. The first peak was prominent (*khl* = 100) whereas the second (*khl* = 110) was weaker but evident. The d_{100} values for the modified aluminas are given in Table 1 along with the corresponding 110 unit cell parameter, *a*, using the equation $a = 2d_{100}/\sqrt{3}$. Accordingly, *a* values amounting to 6.6 and 6.7 nm for the 1 and 3 mol modified aluminas were obtained. The pore diameter can be calculated, as common, from the unit cell parameter *a* value by subtracting 1.0 nm which is an approximate value for the pore wall thickness. Accordingly, pore diameters amounting to 5.6 and 5.7 nm for the 1 and 3 mol modified aluminas, are shown in Fig. 5 (top), which are in good agreement with the values obtained from nitrogen adsorption as shown below.

Wide angle XRD patterns for the calcined materials, Fig. 5 (bottom), show two weak peaks, at *d* spacing amounting to 0.198 and 0.140 nm, characteristic for weakly crystalline γ-alumina. However, intensity of these peaks was weak and decreased on going from the 1 mol to the 3 mol modified material. Thus, indicating that with the increase of the CTAB ratio more thermally stabilized (less crystalline) material was formed (in terms of retardation of crystallization).

3.4. N_2 adsorption isotherm

Nitrogen adsorption isotherms for the 1 and 3 mol calcined materials are shown in Fig. 6 (top). The isotherms can be classified as type IV type of isotherm, and similar to those obtained for mesoporous aluminas prepared by some other recent methods [14,15]. Specific surface areas, S_{BET}, amount to 229 and 348 $m^2\ g^{-1}$ were calculated, respectively, for the 1 and 3 mol calcined materials. Total pore volume, V_p, amounting to 0.230 and 0.416 $cm^3\ g^{-1}$, respectively, were obtained for the 1 mol and 3 mol calcined materials. Pore width, P_w, distributions obtained with the calcined materials are shown in Fig. 6 (bottom). For the calcined 1 mol material a distribution maximize at 3.2 nm (major) and 5.5 nm

Table 1
Texture characteristics for the prepared alumina materials along with some other alumina materials prepared by relevant methods for purpose of comparison

Materials and calcination	S_{BET} ($m^2\ g^{-1}$)	c_{BET}	V_p ($cm^3\ g^{-1}$)	d_{100} (nm)	V_p ($cm^3\ g^{-1}$)	Pore width, P_w (nm)		
						Average	BJH	XRD
1 mol 600 °C/3 h	229	15	0.230	5.72	0.230	4.0	3.2, 5.5	5.6
3 mol 600 °C/3 h	348	109	0.416	5.85	0.416	4.8	3.6, 5.5	5.7
a (303) 550 °C/3 h	310				0.68		7.2	
b (373) 550 °C/3 h	337				0.46		6.7	

a and *b*, mesoporous alumina prepared from cationic surfactants (CTAB) and controlled amounts of water. Molar composition of the mixture, surfactant: Al tri-sec-butoxide:H_2O:1-butanol = 0.5:1:2:10, prepared by hydrothermal treatment for 24 h at 303 K (a) and at 373 K (b), the materials calcined at 550 °C for 3 h, Ref. [15].

(minor) was obtained. A Similar P_w distribution maximize at 3.6 nm (minor) and 5.5 nm (major) was obtained with the 3 mol calcined materials. The increasing of porosity with the development of the second peak and its consistence at the same value (5.5 nm) on going from 1 to 3 mol material may reflect its association with the presence of the CTAB surfactant. Moreover, the increasing of adsorption capacity for the calcined 3 mol than the 1 mol calcined material can be explained in terms of the increased porosity that created by increasing of the surfactant ratio during preparation of the material. Results for the calcined 0 mol material (prepared with no CTAB) showed irreversible type II isotherm with type H3 hysteresis, i.e. type IIb isotherm according to the extended isotherms classification [29]. Moreover, S_{BET} was amounting to 148 $m^2\ g^{-1}$; V_p was amounting to 0.718 $m^3\ g^{-1}$; and BJH P_w distribution was maximizing at 20.3 nm.

The above data showed that both of acetic acid and CTAB have reacted interactively with aluminum alkoxide during its hydrolysis, and subsequently have removed completely during calcinations course. The effect of acetic acid on the hydrolysis of aluminum isopropoxide may be due to formation of bi-dentate ligands, which facilitate networking and/or gelling of the hydrolysis product. Moreover, due to the presence of CTAB in the reaction media during the gel formation, CTAB micelles have incorporated within the gel and thereby facilitate the process of template formation. Results showed that the ordered structure was strong enough to undergo calcinations and template removing process. Texture characteristics of the prepared mesoporous materials are comparable with those recently prepared by other researchers, e.g. mesoporous alumina prepared from cationic surfactants (CTAB) and controlled amounts of water [15], as shown for materials *a* and *b* in Table 1. Moreover, the present texture characteristics are comparable with those reported for mesoporous alumina obtained by a three step sol–gel method [14], in which γ-Al_2O_3 nanocrystals has been synthesized in acid medium with cationic surfactants (CTAB) and in the absence of hydrolysis retarding agents. Where, BET surface areas larger than 300 $m^2\ g^{-1}$, pore diameters within the 4–15 nm range and pore volumes larger than 0.40 $cm^3\ g^{-1}$, were obtained.

4. Conclusions

Simple method for the formation of mesoporous alumina at room temperature was presented. Thereby, mesoporous alumina was produced, reasonable ordering was evident from the low angle XRD which showed two clear peaks for the *hkl* = 100 and 110 planes, whereas most of the other reported materials show only the first peak. Highly amorphous alumina was formed as reflected by the high angle XRD patterns. Moreover, High surface area and relatively narrow pore size distribution was observed. Furthermore, the present method can be employed in preparation of mesoporous alumina powders or surface modification of other materials.

References

[1] K.M.S. Khalil, J. Catal. 178 (1998) 198.
[2] K.M.S. Khalil, J. Colloid Interface Sci. 307 (2007) 172.
[3] G. Øye, W.R. Glomm, T. Vrålstad, S. Volden, H. Magnusson, M. Stöcker, J. Sjöblom, Adv. Colloid Interface Sci. 123–126 (2006) 17–32.
[4] J.C. Ray, K.-S. You, J.-W. Ahn, W.-S. Ahn, Micropor. Mesopor. Mater. 100 (2007) 183.
[5] Z. Gan, G. Ning, Y. Lin, Y. Cong, Mater. Lett. 61 (2007) 3758.
[6] X. Zhag, F. Zhag, K.-Y. Chan, Mater. Lett. 58 (2004) 2872.
[7] M. Yada, M. Machida, T. Kijma, Chem. Commun. (1996) 769.
[8] M. Yada, H. Hiyoshi, K. Ohe, M. Machida, T. Kijma, Inorg. Chem. 36 (1997) 5565.
[9] M. Yada, H. Kitamura, M. Machida, T. Kijima, Langmuir 13 (1997) 5252.
[10] L. Sicard, B. Lebeau, J. Patarin, R. Zana, Langmuir 18 (2002) 74.
[11] A. Caragheorgheopol, H. Caldararu, M. Vasilescu, A. Khan, D. Angelescu, N. Zilkova, J. Phys. Chem. B 108 (2004) 7735.
[12] S. Cabrera, J.E. Haskouri, J. Alamo, A. Beltran, D. Beltran, S. Mendioroz, M.D. Marcos, P. Amoros, Adv. Mater. 11 (1999) 379.
[13] W. Deng, M.W. Toepke, B.H. Shanks, Adv. Funct. Mater. 13 (2003) 61.
[14] J. Aguado, J.M. Escola, M.C. Castro, B. Paredes, Micropor. Mesopor. Mater. 83 (2005) 181.
[15] H.C. Lee, H.J. Kim, C.H. Rhee, K.H. Lee, J.S. Lee, S.H. Chung, Micropor. Mesopor. Mater. 79 (2005) 61.
[16] S.A. Bagshaw, E. Prouzet, T.J. Pinnavaia, Science 269 (1995) 1242.
[17] S.A. Bagshaw, T.J. Pinnavaia, Angew. Chem. Int. Ed. Engl. 35 (1996) 1102.
[18] B.J. Xu, T.C. Xiao, Z.F. Yan, X. Sun, J. Sloan, S.L. González-Cortés, F. Alshahrani, M.L.H. Green, Micropor. Mesopor. Mater. 91 (2006) 293.
[19] Q. Liu, A.Q. Wang, X.D. Wang, T. Zhang, Micropor. Mesopor. Mater. 92 (2006) 10.
[20] L. Ji, J. Lin, K.L. Tan, H.C. Zeng, Chem. Mater. 12 (2000) 931.
[21] F. Vaudry, S. Khodabandeh, M.E. Davis, Chem. Mater. 8 (1996) 1451.
[22] Q. Liu, A. Wang, X. Wang, T. Zhang, Micropor. Mesopor. Mater. 100 (2007) 35.
[23] JCPDS, International Centre for Diffraction Data, PCPDFWIN, 1995 JCPDS-ICDD.
[24] K.S.W. Sing, D.H. Everett, R.A.W. Haul, L. Moscou, R.A. Pierotti, J. Rouquerol, T. Siemieniewska, International Union of Pure and Applied Chemistry, IUPAC, Pure Appl. Chem. 57 (1985) 603.
[25] B. Brunauer, P.H. Emmett, P.H.E. Teller, J. Am. Chem. Soc. 60 (1938) 309.
[26] E.P. Barrett, L.G. Joyner, P.H. Halenda, J. Am. Chem. Soc. 73 (1951) 373.
[27] K.M.S. Khalil, J. Colloid Interface Sci. 315 (2007) 562.
[28] I.A. Degen, Tables of characteristic group frequencies for the interpretation of infrared and Raman spectra, Acolyte Publication, Harrow, UK, 1997.
[29] F. Rouquerol, J. Rouquerol, K. Sing, Adsorption by Powders and Porous Solids, Academic Press, London, 1999, pp. 440–443.